

Distributed Channel Estimation for 6D Movable Antenna: Unveiling Directional Sparsity

Xiaodan Shao, *Member, IEEE*, Rui Zhang, *Fellow, IEEE*, Qijun Jiang, Jihong Park, *Member, IEEE*, Tony Q. S. Quek, *Fellow, IEEE*, and Robert Schober, *Fellow, IEEE*

Abstract—Six-dimensional movable antenna (6DMA) is an innovative and transformative technology to improve wireless network capacity by adjusting the 3D positions and 3D rotations of distributed antenna surfaces based on the channel spatial distribution. In order to achieve optimal antenna positions and rotations, the acquisition of statistical channel state information (CSI) is essential for 6DMA systems. However, the existing works on 6DMA have assumed a central processing unit (CPU) to jointly process the signals of all distributed 6DMA surfaces to execute various tasks such as signal precoding/detection. This inevitably incurs prohibitively high processing cost and latency for channel estimation due to the vast numbers of 6DMA candidate positions/rotations and antenna elements. To tackle this issue, we propose in this paper a distributed 6DMA processing architecture to reduce the processing complexity of the CPU by equipping each 6DMA surface with a local processing unit (LPU). For the new hybrid architecture comprising the CPU and distributed LPUs, we propose new and efficient designs for 6DMA channel acquisition and position/rotation optimization. In particular, we unveil for the first time a new *directional sparsity* property of the 6DMA channels for the distributed users in the system, where each user has significant channel gains only for a (small) subset of 6DMA position-rotation pairs, which can receive direct/reflected signals from the users. In addition, we propose a practical three-stage protocol for the 6DMA-equipped base station (BS) to conduct statistical CSI acquisition for all 6DMA candidate positions/rotations, 6DMA position/rotation optimization, and instantaneous channel estimation for user data transmission with optimized 6DMA positions/rotations. Specifically, the directional sparsity of 6DMA channels is exploited to design distributed algorithms for joint directional sparsity detection and channel power estimation for statistical CSI acquisition, as well as for directional sparsity-aided instantaneous channel estimation. Using the estimated channel power, we further develop a channel power-based optimization algorithm to maximize the ergodic sum rate of the users by optimizing the positions/rotations of the distributed 6DMA surfaces at the BS, subject to practical discrete movement constraints. Simulation results show that the proposed channel estimation algorithms achieve higher accuracy

than several benchmark schemes, while requiring a lower pilot overhead. Furthermore, it is shown that our proposed statistical channel power-based optimization for discrete 6DMA surface positions and rotations outperforms fixed-position antennas and fluid/movable antenna systems with two-dimensional (2D) antenna position optimization only, even if the latter have perfect instantaneous CSI.

Index Terms—Six-dimensional movable antenna (6DMA), distributed 6DMA processing, directional sparsity, joint directional sparsity detection and channel power estimation, statistical channel state information (CSI), antenna position and rotation optimization.

I. INTRODUCTION

As the successor to today's fifth-generation (5G) wireless network, the forthcoming six-generation (6G) wireless network is expected to bring revolutionary advancements, including enormous data speed, improved reliability, minimal latency, extreme connectivity, ubiquitous coverage, and enhanced intelligence and sensing capabilities. To achieve these ambitious goals, the trend is to equip base stations (BSs) and the networks with more antennas, evolving from massive multiple-input multiple-output (MIMO) [1]–[3] to cell-free massive MIMO [4], extremely large-scale MIMO [5], [6], and intelligent reflecting surface (IRS)/reconfigurable intelligent surface (RIS)-aided MIMO [7]–[10]. However, this approach leads to higher hardware costs, increased energy consumption, and greater complexity, which may not meet the performance needs of future wireless networks. A key drawback of current MIMO systems is the fixed positioning of antennas at BSs. With fixed-position antennas (FPAs), the network cannot adapt its resources to varying channel conditions, which limits its ability to adapt to changes in users' three-dimensional (3D) spatial distribution.

Recently, to fully exploit the spatial variation of wireless channels at the transmitter/receiver, six-dimensional movable antenna (6DMA) comprised of multiple rotatable and positionable antennas/antenna surfaces has been proposed as a new technology to improve the performance of wireless networks without increasing the number of antennas [11]–[14]. As shown in Fig. 1, equipped with distributed 6DMA surfaces to match the spatial user distribution, a 6DMA-equipped transmitter/receiver can adaptively allocate antenna resources in space to maximize the array gain and spatial multiplexing gain while also suppressing interference. This thus significantly enhances the capacity of wireless communication networks. In practice, the positions and rotations of 6DMAs can be adjusted continuously [11] or discretely [12] based on the

X. Shao is with the Institute for Digital Communications, Friedrich-Alexander-University Erlangen-Nurnberg (FAU), 91054 Erlangen, Germany (e-mail: xiaodan.shao@fau.de).

R. Zhang is with School of Science and Engineering, Shenzhen Research Institute of Big Data, The Chinese University of Hong Kong, Shenzhen, Guangdong 518172, China (e-mail: rzhang@cuhk.edu.cn). He is also with the Department of Electrical and Computer Engineering, National University of Singapore, Singapore 117583 (e-mail: elezhang@nus.edu.sg).

Q. Jiang is with the School of Science and Engineering, Chinese University of Hong Kong, Shenzhen, China 518172 (e-mail: qijun-jiang@link.cuhk.edu.cn).

J. Park is with the Singapore University of Technology and Design, Singapore 487372 (e-mail: jihong_park@sutd.edu.sg).

T. Q. S. Quek is with the Singapore University of Technology and Design, Singapore 487372 (e-mail: tonyquek@sutd.edu.sg).

R. Schober is with the Institute for Digital Communications, Friedrich-Alexander-University Erlangen-Nurnberg (FAU), 91054 Erlangen, Germany (e-mail: robert.schober@fau.de).

surface movement mechanism, and they can be optimized with or without prior knowledge of the spatial channel distribution of the users in the network [11], [12]. Moreover, the authors in [14] proposed a 6DMA-aided wireless sensing system, showing that 6DMA can also significantly improve the sensing accuracy compared to existing FPA and fluid/movable antenna systems [15]–[17] for both directive and isotropic antenna radiation patterns.

Although the benefits of 6DMA in wireless communication and sensing systems have been demonstrated, the channel state information (CSI) acquisition problem for 6DMA still remains largely unexplored in the literature. The performance gains of 6DMA-aided communication heavily rely on the matching of the positions and rotations of the distributed 6DMA surfaces to the users' spatial channel distribution [11], [12]. To obtain optimal 6DMA positions and rotations, the CSI of the channels between all 6DMA candidate positions/rotations and all users is essential. However, compared to conventional FPA and fluid/movable antennas, 6DMA channel estimation faces the following new challenges. Firstly, FPA has a finite number of channel coefficients to estimate, which is equal to the product of the numbers of transmit and receive antennas. In contrast, for 6DMA channels, the CSI in a continuous space with a practically vast number of candidate antenna positions and/or rotations needs to be acquired. Secondly, for fluid/movable antennas [15], [16] in a given two-dimensional (2D) space, all antenna positions have the same average channel gain for each user, which facilitates CSI acquisition. However, in 6DMA systems, the channels between a user and different candidate antenna positions/rotations in continuous 3D space generally exhibit significantly different distributions (e.g., consider the channels from a user to two 6DMA surfaces whose normal vector points in the direction and the opposite direction of the user, respectively). This inevitably makes the CSI estimation problem for 6DMA more intricate and more challenging than that for fluid/movable antennas. Due to the above reasons, the methods proposed in the existing literature for channel estimation/acquisition for FPA [2], fluid/movable antennas [16], [18] are not applicable to 6DMA in general, which motivates this paper.

On the other hand, the existing works on 6DMA systems [11]–[14] have assumed a centralized processing architecture, where a central processing unit (CPU) is connected with all distributed 6DMA surfaces to execute various tasks such as signal precoding/detection, as shown in Fig. 1(a). For increasing numbers of antennas and candidate antenna positions/rotations, this centralized processing architecture for 6DMA will have to cope with increasingly higher computational cost and complexity as well as the resulting longer processing delay, which may jeopardize the practical deployment of 6DMA in future wireless networks.

To reduce the computational burden of the CPU, recent works on FPA-based massive MIMO systems have introduced a decentralized baseband processing architecture [19]–[21], where the antennas are divided into multiple antenna clusters, and each cluster is equipped with a local baseband processing unit that typically has much lower computational capabilities and thus a lower cost as compared to the traditional CPU.

Inspired by this approach, we propose in this paper a new distributed 6DMA processing architecture as illustrated in Fig. 1(b), to alleviate the computational complexity of the CPU. Specifically, each 6DMA surface is equipped with a local processing unit (LPU), which carries out various signal processing tasks, such as channel estimation and precoding/combining, independently. All LPUs operate in a decentralized and parallel manner, and they can exchange signals with the CPU for joint signal processing. In this paper, we focus on exploiting the proposed 6DMA distributed processing for distributed CSI acquisition at individual 6DMA surfaces, and leveraging the CPU for implementing 6DMA position/rotation optimization. Compared to the conventional centralized 6DMA processing with a single CPU only, the proposed hybrid 6DMA processing with both the CPU and distributed LPUs can not only offload computational tasks from the CPU, but also reduce the baseband data transmission rate between the distributed 6DMA surfaces and the CPU by leveraging the local computation and baseband signal processing at the LPUs, thus effectively reducing the overall processing cost and latency.

Different from the prior works on 6DMA systems, which either assume known statistical CSI between the BS and the users [11] or do not require any CSI [12], this paper aims to address practical CSI acquisition for 6DMA. Particularly, this paper, for the first time, unveils a unique property of 6DMA channels, which we refer to as directional sparsity, i.e., the fact that each user has significant channel gains only for a (small) subset of 6DMA position-rotation pairs that can receive dominant direct/reflected signals given the user's direction. By exploiting this property, we design new distributed algorithms for estimation of the statistical as well as instantaneous CSI for the users at the 6DMA surfaces. The main contributions of this paper can be summarized as follows.

- First, we present the 6DMA system and channel models as well as the directional sparsity of 6DMA channels, and propose a practical protocol for the operation of a BS equipped with 6DMA surfaces. The proposed protocol consists of three stages. In the first stage, the LPUs independently estimate the statistical CSI of different groups of 6DMA candidate positions and rotations in a parallel manner. In the second stage, based on the estimated statistical CSI, the positions and rotations of all 6DMA surfaces are optimized by the CPU, and then all 6DMA surfaces are moved to their optimized positions and rotations under the joint control of the CPU and their associated LPUs. In the third stage, with the 6DMA surfaces at their optimized positions and rotations, the instantaneous channels of all the users are estimated at the relevant LPUs in a distributed manner by leveraging the directional sparsity determined in the first stage, and all users transmit their data ¹.

¹It is worth noting that in this protocol, user communications take place continuously with no interruption due to the movement of 6DMA surfaces. This is because the movement of the surfaces occurs on a much larger time scale as compared to the coherence time of the instantaneous user channels and consequently, the surfaces' positions and rotations can be assumed to be constant within each channel coherence time.

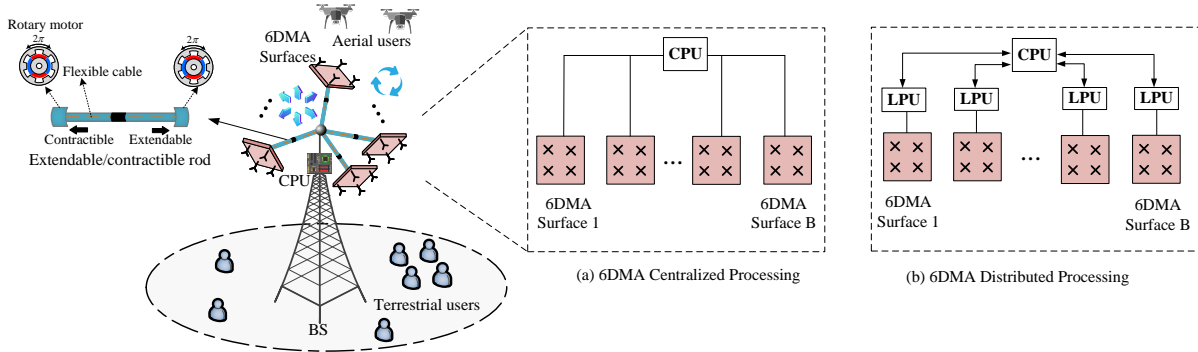


Fig. 1. 6DMA-equipped BS and different processing architectures.

- Moreover, we propose a joint directional sparsity detection and channel power estimation algorithm for the statistical CSI acquisition in the first stage, as well as a directional sparsity-aided instantaneous channel estimation algorithm in the third stage. Using the estimated average channel power, we further develop a channel power-based optimization algorithm for the second stage to maximize the average sum-rate of all users by jointly optimizing the 3D positions and rotations of all 6DMA surfaces at the BS, subject to practical discrete movement constraints.
- Finally, we evaluate the performance of the proposed statistical CSI and instantaneous CSI estimation algorithms for 6DMA by extensive simulations. Our results demonstrate that the proposed schemes can significantly improve the channel estimation accuracy as compared to several benchmark schemes. Moreover, it is shown that the proposed statistical channel power-based 6DMA position/rotation optimization framework outperforms FPA and fluid/movable antenna systems with 2D antenna position optimization only, even if the latter have perfect instantaneous CSI.

The remainder of this paper is organized as follows. Section II presents the 6DMA-BS model with discrete 3D position/rotation adjustment of the 6DMA surfaces and the corresponding channel model, as well as the proposed 6DMA distributed processing architecture. In Section III, we unveil the directional sparsity of 6DMA channels and propose a practical protocol for the operation of the 6DMA-BS. In Sections IV and V, we present the proposed distributed channel estimation algorithms and the proposed position/rotation optimization algorithm, respectively. Section VI provides numerical results and pertinent discussions. Finally, Section VII concludes this paper.

Notations: The symbols $(\cdot)^*$, $(\cdot)^H$, and $(\cdot)^T$ represent the conjugate, conjugate transpose, and transpose, respectively. $\mathbb{E}[\cdot]$ is the expectation. $\|\cdot\|_2$, $\|\cdot\|_F$, and \mathbf{I}_N denote the Euclidean norm, the Frobenius norm, and the $N \times N$ identity matrix, respectively. $\mathbf{1}_{N \times 1}$ represents an all-ones vector with dimensions $N \times 1$. $[\mathbf{a}]_j$ and $[\mathbf{A}]_{i,j}$ represent the j -th element of a vector and the (i, j) element of a matrix, respectively. $\text{tr}(\cdot)$ denotes the trace of a matrix. $\mathcal{O}(\cdot)$ denotes the big-O notation. $\arctan 2(\cdot)$ is the two argument arctangent function. $\text{round}(\mathbf{s})$ denotes the operation that rounds each element of \mathbf{s} to the

nearest integer. \cup denotes the union of two sets. $|\cdot|_c$ denotes the number of elements of a set. Γ^c denotes the complementary set of set Γ .

II. SYSTEM MODEL

A. Distributed 6DMA Architecture

As illustrated in Fig. 1, the proposed 6DMA-BS comprises B distributed 6DMA surfaces, indexed by set $\mathcal{B} = \{1, 2, \dots, B\}$. Each surface is modeled as a uniform planar array (UPA) with $N \geq 1$ antennas, indexed by set $\mathcal{N} = \{1, 2, \dots, N\}$. Each 6DMA surface is equipped with a local computing hardware, i.e., LPU, which carries out the necessary baseband processing tasks, such as channel estimation and signal precoding/combining, in a decentralized and parallel fashion (see Fig. 1(b)). Each LPU is connected to the common CPU at the BS via a separate rod, which houses flexible cables (e.g., coaxial cables). These cables supply power to the 6DMA surface and LPU, and also facilitate control and signal exchange between the LPU and CPU. Moreover, the CPU controls two rotary motors that are mounted at both ends of the rod to adjust the position and rotation of each 6DMA surface. In addition, each rod can flexibly contract and extend to control the distance between each 6DMA surface and the CPU. For this setup, the BS can function akin to a “transformer”, possessing the capability to instantly reconfigure its antenna array into virtually any conceivable shape for optimizing wireless network performance.

For ease of practical implementation, we assume that each 6DMA surface can only adopt a finite set of discrete positions and rotations. For simplicity, we assume that for each candidate position, there is only one possible rotation². We assume that there are in total $M \geq B$ discrete position-rotation pairs $(\mathbf{q}_m, \mathbf{u}_m)$, denoted by set $\mathcal{M} = \{1, 2, \dots, M\}$, where $\mathbf{q}_m \in \mathbb{R}^3, m \in \mathcal{M}$ and $\mathbf{u}_m \in \mathbb{R}^3, m \in \mathcal{M}$, denote the m -th possible discrete position and rotation of the 6DMA surfaces, respectively. They are specified as follows:

$$\mathbf{q}_m = [x_m, y_m, z_m]^T \in \mathcal{C}, \quad (1)$$

$$\mathbf{u}_m = [\alpha_m, \alpha_m, \gamma_m]^T, \quad (2)$$

where x_m, y_m , and z_m are the coordinates of the 6DMA surface’s center at the m -th discrete position in a global Cartesian

²This work can be easily extended to the case where for each position, there are multiple rotations [12].

coordinate system (CCS) with origin o , where the CPU is located. The rotation angles α_m , β_m , and γ_m correspond to rotations around the x -axis, y -axis, and z -axis, respectively. The space \mathcal{C} defines the 3D area at the BS site where the 6DMA surfaces can be dynamically positioned and rotated.

The rotation matrix $\mathbf{R}(\mathbf{u}_m)$ for the angles in \mathbf{u}_m is given by

$$\mathbf{R}(\mathbf{u}_m) = \begin{bmatrix} c_{\alpha_m} c_{\gamma_m} & & c_{\alpha_m} \omega_{\gamma_m} & -\omega_{\alpha_m} \\ \omega_{\alpha_m} \omega_{\alpha_m} c_{\gamma_m} - c_{\alpha_m} \omega_{\gamma_m} & \omega_{\alpha_m} \omega_{\alpha_m} \omega_{\gamma_m} + c_{\alpha_m} c_{\gamma_m} & c_{\alpha_m} \omega_{\alpha_m} & \\ c_{\alpha_m} \omega_{\alpha_m} c_{\gamma_m} + \omega_{\alpha_m} \omega_{\gamma_m} & c_{\alpha_m} \omega_{\alpha_m} \omega_{\gamma_m} - \omega_{\alpha_m} c_{\gamma_m} & \omega_{\alpha_m} \omega_{\alpha_m} & c_{\alpha_m} c_{\alpha_m} \end{bmatrix}, \quad (3)$$

where $c_x = \cos(x)$ and $\omega_x = \sin(x)$ [22]. We set a local CCS for the 6DMA surface at each location, which is shown by $o'-x'y'z'$, with o' being the center of the surface. The position of the n -th antenna on the 6DMA surface in its local CCS is shown by $\bar{\mathbf{r}}_n \in \mathbb{R}^3$. The rotation \mathbf{u}_m and position \mathbf{q}_m are then used to find the position of the n -th antenna on the 6DMA surface at the m th discrete position in the global CCS. This is given by $\mathbf{r}_{m,n} \in \mathbb{R}^3$ as follows:

$$\mathbf{r}_{m,n}(\mathbf{q}_m, \mathbf{u}_m) = \mathbf{q}_m + \mathbf{R}(\mathbf{u}_m) \bar{\mathbf{r}}_n, \quad n \in \mathcal{N}, \quad m \in \mathcal{M}. \quad (4)$$

We define $\mathcal{Q} = \{(\mathbf{q}_1, \mathbf{u}_1), (\mathbf{q}_2, \mathbf{u}_2), \dots, (\mathbf{q}_M, \mathbf{u}_M)\}$ as the set of M discrete position-rotation pairs for the 6DMA surfaces. Let $i_b \in \mathcal{M}$ be the index of the chosen position-rotation pair for the b -th 6DMA surface, $b \in \mathcal{B}$. Thus, the position-rotation pair for the b -th surface is $(\mathbf{q}_{i_b}, \mathbf{u}_{i_b}) \in \mathcal{Q}$. As explained in [11], [12], the following three practical constraints for rotating/positioning 6DMA surfaces need to be considered:

$$\mathbf{n}(\mathbf{u}_{i_b})^T (\mathbf{q}_{i_j} - \mathbf{q}_{i_b}) \leq 0, \quad \forall b, j \in \mathcal{B}, j \neq b, \quad (5)$$

$$\mathbf{n}(\mathbf{u}_{i_b})^T \mathbf{q}_{i_b} \geq 0, \quad \forall b \in \mathcal{B}, \quad (6)$$

$$\|\mathbf{q}_{i_b} - \mathbf{q}_{i_j}\|_2 \geq d_{\min}, \quad \forall b, j \in \mathcal{B}, j \neq b, \quad (7)$$

where vector $\mathbf{n}(\mathbf{u}_{i_b}) = \mathbf{R}(\mathbf{u}_{i_b}) \bar{\mathbf{n}}$ represents the normal vector of the b -th 6DMA surface in the global CCS, with $\bar{\mathbf{n}}$ being its local CCS counterpart. d_{\min} is the minimum distance allowed between any two 6DMA surfaces to prevent overlapping and coupling. Constraint (5) prevents mutual signal reflections between surfaces, while constraint (6) ensures that the CPU does not block the signal of the 6DMA surfaces.

B. Channel Model

We focus on uplink multiuser transmission, where K users, each equipped with a single FPA, are spatially distributed throughout the cell. Assuming the presence of a multipath channel between each user and the BS, the channel from user k to the B 6DMA surfaces, represented as $\mathbf{h}_k(\mathbf{q}, \mathbf{u}) \in \mathbb{C}^{NB \times 1}$, is defined as follows:

$$\mathbf{h}_k(\mathbf{q}, \mathbf{u}) = [\mathbf{h}_{1,k}^T(\mathbf{q}_{i_1}, \mathbf{u}_{i_1}), \dots, \mathbf{h}_{B,k}^T(\mathbf{q}_{i_B}, \mathbf{u}_{i_B})]^T, \quad (8)$$

with

$$\mathbf{q} = [\mathbf{q}_{i_1}^T, \mathbf{q}_{i_2}^T, \dots, \mathbf{q}_{i_B}^T]^T \in \mathbb{R}^{3B \times 1}, \quad (9)$$

$$\mathbf{u} = [\mathbf{u}_{i_1}^T, \mathbf{u}_{i_2}^T, \dots, \mathbf{u}_{i_B}^T]^T \in \mathbb{R}^{3B \times 1}. \quad (10)$$

In (8), $\mathbf{h}_{b,k}(\mathbf{q}_{i_b}, \mathbf{u}_{i_b}) \in \mathbb{C}^{N \times 1}$ represents the channel from the k -th user to all the antennas of the b -th 6DMA surface at the 6DMA-BS, and can be expressed as

$$\mathbf{h}_{b,k}(\mathbf{q}_{i_b}, \mathbf{u}_{i_b}) = \sum_{\ell=1}^{\Gamma_k} \mu_{\ell,k} \sqrt{g_{\ell,k}(\mathbf{u}_{i_b})} \mathbf{a}_{\ell,k}(\mathbf{q}_{i_b}, \mathbf{u}_{i_b}), \quad (11)$$

where Γ_k represents the total number of channel paths from user k to the BS, and $\mu_{\ell,k}$ denotes the channel coefficient from user k to the CPU along path ℓ .

The 6D steering vector of the b -th 6DMA surface for receiving a signal from user k over path ℓ is expressed as follows:

$$\begin{aligned} & \mathbf{a}_{\ell,k}(\mathbf{q}_{i_b}, \mathbf{u}_{i_b}) \\ &= \left[e^{-j \frac{2\pi}{\lambda} \mathbf{f}_{\ell,k}^T \mathbf{r}_{i_b,1}(\mathbf{q}_{i_b}, \mathbf{u}_{i_b})}, \dots, e^{-j \frac{2\pi}{\lambda} \mathbf{f}_{\ell,k}^T \mathbf{r}_{i_b,N}(\mathbf{q}_{i_b}, \mathbf{u}_{i_b})} \right]^T, \end{aligned} \quad (12)$$

where λ denotes the carrier wavelength, and $\mathbf{f}_{\ell,k}$ represents the pointing vector corresponding to direction $(\theta_{\ell,k}, \phi_{\ell,k})$, which is defined as

$$\mathbf{f}_{\ell,k} = [\cos(\theta_{\ell,k}) \cos(\phi_{\ell,k}), \cos(\theta_{\ell,k}) \sin(\phi_{\ell,k}), \sin(\theta_{\ell,k})]^T, \quad (13)$$

where the azimuth and elevation angles for the ℓ -th channel path between user k and the BS are given by $\phi_{\ell,k} \in [-\pi, \pi]$ and $\theta_{\ell,k} \in [-\pi/2, \pi/2]$, respectively. The effective antenna gain of the b -th 6DMA surface along direction $(\tilde{\theta}_{b,\ell,k}, \tilde{\phi}_{b,\ell,k})$ in the linear scale is defined as follows:

$$g_{\ell,k}(\mathbf{u}_{i_b}) = 10^{\frac{A(\tilde{\theta}_{b,\ell,k}, \tilde{\phi}_{b,\ell,k})}{10}}, \quad b \in \mathcal{B}, \ell \in \Gamma_k, k \in \mathcal{K}, \quad (14)$$

with

$$\tilde{\theta}_{b,\ell,k} = \pi/2 - \arccos(\tilde{z}_{b,\ell,k}), \quad (15)$$

$$\tilde{\phi}_{b,\ell,k} = \arccos\left(\frac{\tilde{x}_{b,\ell,k}}{\sqrt{\tilde{x}_{b,\ell,k}^2 + \tilde{y}_{b,\ell,k}^2}}\right) \times \tau(\tilde{y}_{b,\ell,k}), \quad (16)$$

$$[\tilde{x}_{b,\ell,k}, \tilde{y}_{b,\ell,k}, \tilde{z}_{b,\ell,k}]^T = -\mathbf{R}(\mathbf{u}_{i_b})^T \mathbf{f}_{\ell,k}, \quad (17)$$

$$\tau(\tilde{y}_{b,\ell,k}) = \begin{cases} 1, & \tilde{y}_{b,\ell,k} \geq 0, \\ -1, & \tilde{y}_{b,\ell,k} < 0, \end{cases} \quad (18)$$

where $A(\tilde{\theta}_{b,\ell,k}, \tilde{\phi}_{b,\ell,k})$ denotes the effective antenna gain in dBi, which is determined by the radiation pattern of the selected antenna.

It is worth noting that the 6DMA channel in (11) is a function of the positions and rotations of all 6DMA surfaces, indicating that the channel quality can be adjusted by positioning and rotating the 6DMA surfaces. To reconfigure the positions and rotations of the 6DMA surfaces and obtain a desired channel quality, accurate statistical CSI between all the users and the M 6DMA candidate position-rotation pairs is required.

C. Achievable Sum Rate Analysis

The multiple-access channel from the K users to a 6DMA surface at all possible discrete positions and rotations is characterized by $\mathbf{H} = [\mathbf{H}_1^T, \dots, \mathbf{H}_M^T]^T \in \mathbb{C}^{MN \times K}$ with $\mathbf{H}_m = [\mathbf{h}_{m,1}(\mathbf{q}_m, \mathbf{u}_m), \dots, \mathbf{h}_{m,K}(\mathbf{q}_m, \mathbf{u}_m)] \in \mathbb{C}^{N \times K}$, $m \in \mathcal{M}$, (19)

denoting the channel from all K users to all the antennas of the m -th 6DMA candidate position-rotation pair. In addition, we denote

$$\bar{\mathbf{H}}(\mathbf{q}, \mathbf{u}) = [\mathbf{h}_1(\mathbf{q}, \mathbf{u}), \mathbf{h}_2(\mathbf{q}, \mathbf{u}), \dots, \mathbf{h}_K(\mathbf{q}, \mathbf{u})] \in \mathbb{C}^{BN \times K}, \quad (20)$$

as the multiple-access channel from all K users to all B 6DMA surfaces at the BS (given fixed corresponding position-

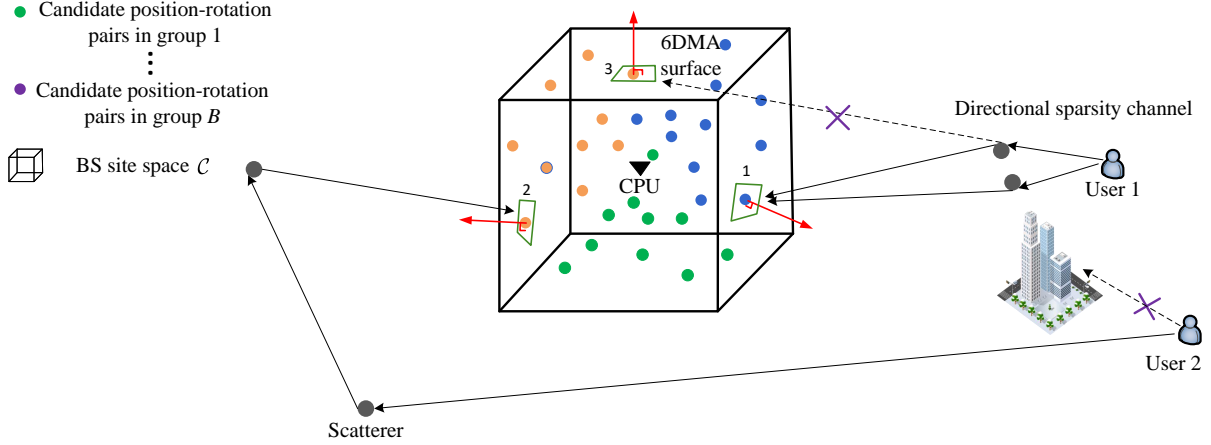


Fig. 2. Illustration of the directional sparsity of 6DMA channels and the 6DMA candidate position-rotation pair grouping.

rotation pairs). It can be shown that $\bar{\mathbf{H}}(\mathbf{q}, \mathbf{u})$ can be expressed in terms of \mathbf{H} as

$$\bar{\mathbf{H}}(\mathbf{q}, \mathbf{u}) = (\mathbf{S} \otimes \mathbf{I}_N) \mathbf{H}, \quad (21)$$

where $\mathbf{S} \in \mathbb{R}^{B \times M}$ is the position/rotation selection matrix, which is defined by

$$[\mathbf{S}]_{b,m} = \begin{cases} 1, & \text{if the } b\text{-th 6DMA surface selects candidate} \\ & \text{position-rotation pair } m, \\ 0, & \text{otherwise,} \end{cases} \quad (22)$$

for $b \in \mathcal{B}$ and $m \in \mathcal{M}$.

Then, the received signals at the BS are given by

$$\mathbf{y} = (\mathbf{S} \otimes \mathbf{I}_N) \mathbf{H} \bar{\mathbf{x}} + \mathbf{w}, \quad (23)$$

where $\mathbf{w} \sim \mathcal{CN}(\mathbf{0}_{NB}, \sigma^2 \mathbf{I}_{NB})$ denotes the complex additive white Gaussian noise (AWGN) vector at the BS with zero mean and average power σ^2 . In the above, $\bar{\mathbf{x}} = \sqrt{p}[\bar{x}_1, \bar{x}_2, \dots, \bar{x}_K]^T \in \mathbb{C}^{K \times 1}$, where \bar{x}_k is the normalized transmit signal of user k with unit average power, and p denotes the transmit power for each user.

Based on (23) and by applying the expectation w.r.t. the random channel \mathbf{H} , the achievable ergodic sum rate of the users is given by [23]

$$C(\mathbf{s}) = \mathbb{E} \left[\log_2 \det \left(\mathbf{I}_K + \frac{p}{\sigma^2} \mathbf{H}^H (\mathbf{S} \otimes \mathbf{I}_N)^T (\mathbf{S} \otimes \mathbf{I}_N) \mathbf{H} \right) \right] \quad (24)$$

$$= \mathbb{E} \left[\log_2 \det \left(\mathbf{I}_K + \frac{p}{\sigma^2} \mathbf{H}^H (\text{diag}(\mathbf{s}) \otimes \mathbf{I}_N) \mathbf{H} \right) \right], \quad (25)$$

where (25) holds as $(\mathbf{S} \otimes \mathbf{I}_N)^T (\mathbf{S} \otimes \mathbf{I}_N) = \text{diag}(\mathbf{s}) \otimes \mathbf{I}_N$, with $\mathbf{s} \in \mathbb{R}^{M \times 1}$ being the position/rotation selection vector defined as follows:

$$[\mathbf{s}]_m = \begin{cases} 1, & \text{if position-rotation pair } m \text{ is selected} \\ & \text{for a 6DMA surface,} \\ 0, & \text{otherwise,} \end{cases} \quad (26)$$

for $m \in \mathcal{M}$.

The exact ergodic sum rate in (25) is hard to obtain, hence we resort to deriving an upper bound for it by exploiting the Jensen's inequality, which will be used in the subsequent optimization. Assuming that the channels between users are statistically independent, an upper bound of $C(\mathbf{s})$ in (25) can

be obtained as

$$\begin{aligned} C(\mathbf{s}) &\leq \bar{C}(\mathbf{s}) \\ &= \log_2 \det \left(\mathbf{I}_K + \frac{p}{\sigma^2} \mathbb{E} \left[\mathbf{H}^H (\text{diag}(\mathbf{s}) \otimes \mathbf{I}_N) \mathbf{H} \right] \right) \quad (27) \\ &= \log_2 \det \left(\mathbf{I}_K + \frac{p}{\sigma^2} \mathbb{E} \left[\sum_{m=1}^M [\mathbf{s}]_m \sum_{j=N(m-1)+1}^{Nm} [\mathbf{H}]_{j,:}^H [\mathbf{H}]_{j,:} \right] \right) \quad (28) \\ &= \sum_{k=1}^K \log_2 \left(1 + \frac{p}{\sigma^2} \sum_{m=1}^M [\mathbf{s}]_m \sum_{j=N(m-1)+1}^{Nm} \mathbb{E} [|[\mathbf{H}]_{j,k}|^2] \right) \quad (29) \end{aligned}$$

$$= \sum_{k=1}^K \log_2 \left(1 + \frac{p}{\sigma^2} \sum_{m=1}^M [\mathbf{s}]_m [\mathbf{P}]_{m,k} \right), \quad (30)$$

where (28) holds due to the assumed independence of the channels of different users, and $\mathbf{P} \in \mathbb{R}^{M \times K}$ represents the average channel power matrix, with its (m, k) -th element, $\sum_{j=N(m-1)+1}^{Nm} \mathbb{E} [|[\mathbf{H}]_{j,k}|^2]$, denoting the average power of the channels between user k and all antennas on a 6DMA surface located at candidate position-rotation pair m .

It is worth noting that different from the conventional multi-user channel with FPAs, the ergodic sum rate with 6DMAs depends on the candidate position/rotation statistical CSI (average power distribution), \mathbf{P} , and position/rotation selection vector \mathbf{s} , which underlines the importance of estimating the candidate position/rotation's statistical CSI \mathbf{P} , as only for \mathbf{P} known, the position/rotation selection \mathbf{s} can be optimized to maximize the ergodic sum rate.

III. DIRECTIONAL SPARSITY AND PROTOCOL DESIGN

In this section, we introduce the peculiar directional sparsity property of 6DMA channels and propose a practical protocol for the operation of the 6DMA-BS with distributed signal processing.

A. Directional Sparsity of 6DMA Channels

In existing wireless networks, the BS is usually installed at a high altitude. Thus, there are only a limited number of scatterers around the BS, while there may be rich scatterers near

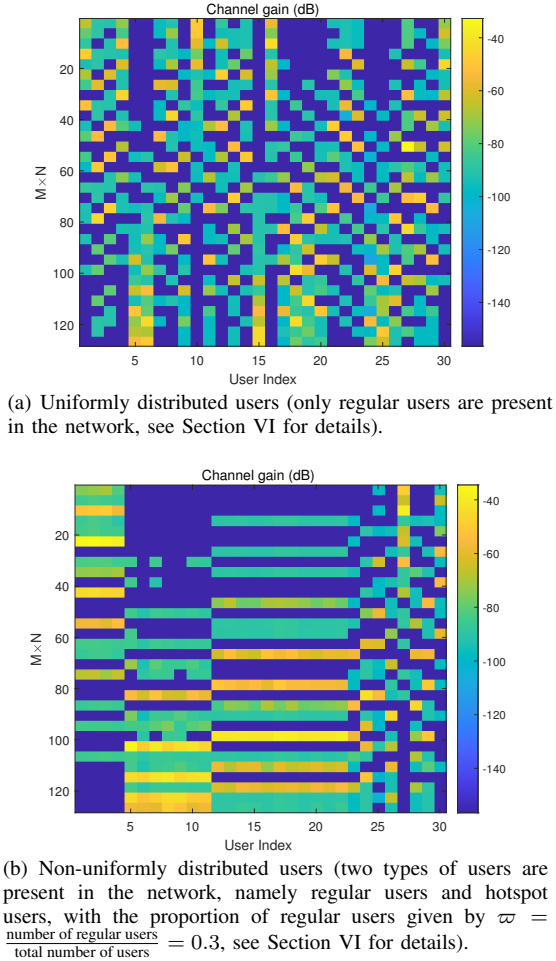


Fig. 3. An illustration of the sparse pattern in \mathbf{H} .

each of the users. Due to the rotatability, positionability, and antenna directivity of 6DMA, the channels between a given user and different candidate 6DMA positions and rotations in a continuous 3D space generally exhibit drastically different distributions. In this case, each user k may have channels with significant gains only for a small subset of 6DMA position-rotation pairs indexed by the set $\mathcal{W}_k \subseteq \mathcal{M}$. While for the remaining candidate position-rotation pairs $m \in \mathcal{W}_k^c$, which may either face in the opposite direction of the user or be blocked by obstacles towards the user, the effective channels of the user are much weaker and thus can be ignored. For example, in Fig. 2, user 1 can establish a significant channel with candidate position-rotation pair 1, but its channels with candidate position-rotation pairs 2 and 3 are much smaller and thus can be assumed to be approximately zero. This leads to sparsity in the channels between the users and different 6DMA position-rotation pairs, which we define as *directional sparsity* as follows.

Definition 1 (Directional Sparsity): In the considered 6DMA channel model in (11), user k is assumed to have positive channel gains to only a subset of 6DMA position-rotation pairs $m \in \mathcal{W}_k$ (i.e., the corresponding antenna gain $g_{l,k}(\mathbf{u}_m) \neq 0, m \in \mathcal{W}_k$, in (11)); while for the remaining 6DMA position-rotation pairs $m \in \mathcal{W}_k^c$, the channels to user

k are assumed to be zero (i.e., $g_{l,k}(\mathbf{u}_m) = 0, m \in \mathcal{W}_k^c$, in (11)).

An illustration of the directional sparsity of the 6DMA channels from the K users to all 6DMA discrete position-rotation pairs, i.e., $\mathbf{H} \in \mathbb{C}^{MN \times K}$, is provided in Fig. 3³. It is interesting to observe that the channel gains of \mathbf{H} exhibit a ‘*block sparsity*’ pattern, for both the cases of uniform and non-uniform user distributions. This is due to the directional sparsity for each user’s channels to all candidate position-rotation pairs as well as the fact that all N antennas of a 6DMA surface for a given position-rotation pair have the same channel power distribution.

To characterize the directional sparsity of 6DMA channels, we define $\mathbf{Z} \in \mathbb{R}^{M \times K}$ as the directional sparsity indicator matrix with $[\mathbf{Z}]_{m,k} = 1$ if the k -th user w.r.t. a 6DMA surface located at the m -th candidate position-rotation pair has a positive channel power, and $[\mathbf{Z}]_{m,k} = 0$ otherwise. Thus, we have

$$[\mathbf{Z}]_{m,k} = \begin{cases} 1, & \text{if the channel between the } k\text{-th user} \\ & \text{and the } m\text{-th candidate 6DMA} \\ & \text{position-rotation is non-zero,} \\ 0, & \text{otherwise.} \end{cases} \quad (31)$$

Note that the proposed simplified channel model is applicable to 6DMA channels only due to their unique directional sparsity. It is also worth noting that the directional sparsity in the context of 6DMA is different from the traditional concept of angular channel sparsity in MIMO systems with FPAs [2], which generally refers to the scenario where the number of dominant channel paths from each user is significantly smaller than the number of FPAs at the transmitter/receiver, regardless of their positions/rotations.

B. Protocol Design

Next, we propose a practical protocol for the operation of the 6DMA-BS, as illustrated in Fig. 4. The protocol consists of the following three stages in each long transmission frame.

- Stage I (Candidate position/rotation statistical CSI (i.e., joint directional sparsity detection and channel power) estimation): In the long transmission frame, we assume that the statistical CSI between all 6DMA candidate position-rotation pairs and all users remains constant. Thus, we can estimate the statistical CSI in terms of the directional sparsity matrix \mathbf{Z} and the average channel power matrix \mathbf{P} (see Section IV-A for details) in Stage I. Specifically, the 6DMA surface moves over $\bar{M} < M$ different position-rotation pairs to collect data for estimating the statistical CSI of these \bar{M} position-rotation pairs. To reduce the CPU processing complexity and the baseband signal transmission rate between 6DMA surfaces and the CPU, we propose dividing the \bar{M} position-rotation pairs into B groups (see Fig. 2), with each group containing $M_g = \bar{M}/B$ different position-rotation pairs⁴.

³Note that the directional sparsity applies not only to $\mathbf{H} \in \mathbb{C}^{MN \times K}$, but also to the 6DMA channel $\mathbf{H}(\mathbf{q}, \mathbf{u}) \in \mathbb{C}^{BN \times K}$, where the B 6DMA surfaces select B out of the M candidate position-rotation pairs.

⁴We assume that \bar{M} is divisible by B for convenience.

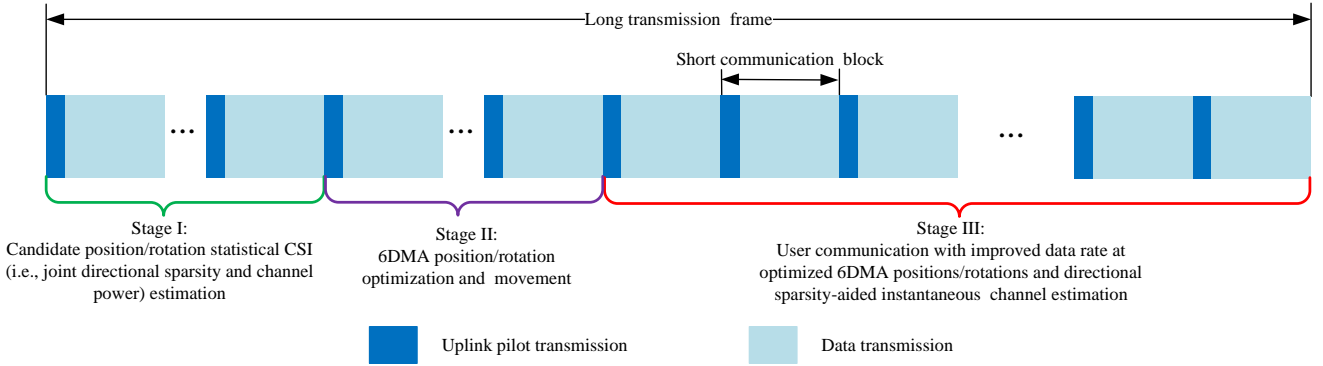


Fig. 4. The proposed three-stage protocol for 6DMA system.

Each 6DMA surface is assigned to a different group and it moves to all M_g different positions-rotations pairs within that group, while its LPU collects the uplink pilot signals received from the users (which have non-zero channels with it). Then, all LPUs independently estimate the statistical CSI for different groups of M_g 6DMA position-rotation pairs in parallel. Subsequently, we can reconstruct the statistical CSI for any position-rotation pair in BS site region \mathcal{C} , based on the previously estimated statistical CSI for a finite number of \bar{M} position-rotation pairs. Note that user communications take place continuously with no interruption due to the movement of 6DMA surfaces in this stage.

- Stage II (6DMA position/rotation optimization and movement): After Stage I, all LPUs send their locally estimated candidate position/rotation statistical CSI to the CPU. With the global statistical CSI, the CPU of the 6DMA-BS then optimizes the positions and rotations of all B 6DMA surfaces in this stage to maximize the ergodic sum rate (see Section V for details). Once the optimized positions and rotations of the 6DMA surfaces have been determined, the 6DMA surfaces are gradually moved over consecutive communication blocks to the optimized positions and rotations. Note that, similar to Stage I, user communications continue uninterruptedly during this stage despite the movement of the 6DMA surfaces. This is because the movement of these surfaces occurs on a much larger time scale as compared to the coherence time of instantaneous user channels, and consequently, the positions/rotations of 6DMA surfaces can be assumed to be constant within each channel's coherence time (see Fig. 4).
- Stage III (User communication with improved data rate at optimized 6DMA positions/rotations and directional sparsity-aided instantaneous channel estimation): With all 6DMA surfaces located at their optimized positions and rotations in Stage II, the users can communicate with the BS with an improved sum rate, where the instantaneous channels between the users and each 6DMA surface located at its optimized position and rotation can be estimated at the connected LPU in a distributed manner by leveraging the directional sparsity estimated in Stage

I (see Section IV-B for details)⁵.

It is worth noting that in the above proposed protocol, the complicated 6DMA channel acquisition problem is decoupled into the statistical CSI estimation for all candidate positions/rotations and the subsequent instantaneous CSI estimation for all optimized positions/rotations, to exploit the 6DMA channel directional sparsity and reduce the pilot overhead. On the one hand, the candidate position/rotation channel is high-dimensional but statistically constant during the long transmission frame. Thus, the candidate position/rotation statistical CSI can be estimated much less frequently than the candidate position/rotation instantaneous CSI, and the average pilot overhead for the former is low in the long term. On the other hand, for both candidate position/rotation statistical CSI estimation and optimized position/rotation instantaneous CSI estimation, the 6DMA channel directional sparsity can be exploited to further reduce the pilot overhead, as will be shown in the next section in detail.

IV. DISTRIBUTED CHANNEL ESTIMATION ALGORITHMS

In this section, we propose distributed 6DMA channel estimation schemes to acquire the statistical CSI for all candidate 6DMA positions and rotations, and the instantaneous CSI at the optimized 6DMA positions and rotations, as specified in Stages I and III in the proposed protocol (see Fig. 4), respectively.

A. Joint Directional Sparsity Detection and Channel Power Estimation in Stage I

1) *Candidate Position-Rotation Pair Grouping*: The 6DMA surface moves over $\bar{M} < M$ different position-rotation pairs to collect data for estimating the statistical CSI of these \bar{M} position-rotation pairs. Then, the statistical CSI for all available M candidate position-rotation pairs in the BS site region \mathcal{C} can be reconstructed based on the estimated statistical CSI for a finite number of \bar{M} position-rotation pairs. To perform distributed channel estimation, we first divide the \bar{M} position-rotation pairs into B equal-size groups, with each group having $M_g = \frac{\bar{M}}{B}$ position-rotation pairs (see Fig. 2).

⁵Note that the instantaneous channels between users and the B 6DMA surfaces in Stage I and Stage II are also estimated for data communication by using the traditional unlink channel estimation method [1].

The LPU connected to the b -th 6DMA surface is responsible for estimating the channels between all K users and the subset of position-rotation pairs in group b , $b = 1, 2, \dots, B$. In this way, all LPUs can estimate their corresponding channels in parallel, thus reducing the channel estimation complexity and pilot overhead in each group.

2) *Covariance-Based Algorithm*: To enable the directional sparsity detection and average channel power estimation in Stage I of the proposed protocol, we assume that each LPU collects in total L pilot symbols from each user. It is assumed that the pilots from user k , denoted by $\mathbf{x}_k \in \mathbb{C}^{L \times 1}$, are generated following an independent and identically distributed (i.i.d.) complex Gaussian distribution with zero mean and unit variance. Then, for any LPU, the received signal $\mathbf{Y}_m \in \mathbb{C}^{L \times N}$, $m \in \{1, 2, \dots, M_g\}$, at the m -th candidate position-rotation pair can be expressed as

$$\mathbf{Y}_m = \sum_{k=1}^K [\bar{\mathbf{Z}}]_{m,k} \mathbf{x}_k \mathbf{h}_{m,k}^T + \mathbf{W}_m = \mathbf{X} \text{diag}([\bar{\mathbf{Z}}]_{m,:}) \mathbf{H}_m^T + \mathbf{W}_m, \quad (32)$$

where $\bar{\mathbf{Z}} \in \mathbb{R}^{\bar{M} \times K}$ represents the average channel power matrix for \bar{M} position-rotation pairs, $\mathbf{X} = [\mathbf{x}_1, \dots, \mathbf{x}_K] \in \mathbb{C}^{L \times K}$ denotes the horizontal stack of all pilots from all users, and $\mathbf{W}_m \in \mathbb{C}^{L \times M}$ is the AWGN matrix with i.i.d. entries following distribution $\mathcal{CN}(0, \sigma^2)$.

Remark 1: Our goal is to estimate the channel power $\bar{\mathbf{P}}$ and the directional sparsity indicator matrix $\bar{\mathbf{Z}}$ in Stage I as they will be used as the statistical CSI for the subsequent optimization of the positions and rotations of the 6DMA surfaces in Stage II, and for instantaneous CSI estimation in Stage III of the proposed protocol (see Sections IV-B and V for details). One possible approach is to treat (32) as a compressed sensing (CS) model with multiple measurement vectors and exploit the row sparsity of $\hat{\mathbf{H}}_m = \text{diag}([\bar{\mathbf{Z}}]_{m,:}) \mathbf{H}_m^T$. Once $\hat{\mathbf{H}}_m$ is recovered from \mathbf{Y}_m by applying CS-based algorithms, $[\bar{\mathbf{Z}}]_{m,k}$ can be determined from the rows of $\hat{\mathbf{H}}_m$. However, this approach requires a computational complexity that scales with N since $\hat{\mathbf{H}}_m$ is of size $K \times N$, which may be problematic for large N . Moreover, the exact entries of $\hat{\mathbf{H}}_m$ are not required for the subsequent 6DMA position and rotation optimization (as it is based on the statistical CSI of the 6DMA channels), and estimating them would require a high pilot overhead due to the large number of unknowns [24].

Therefore, instead of recovering the exact channel $\hat{\mathbf{H}}_m$, we estimate the power state vector $\boldsymbol{\eta}_m$ (from which $[\bar{\mathbf{Z}}]_{m,k}$ can also be determined), which is defined as

$$\boldsymbol{\eta}_m = [[\bar{\mathbf{P}}]_{m,1} [\bar{\mathbf{Z}}]_{m,1}, [\bar{\mathbf{P}}]_{m,2} [\bar{\mathbf{Z}}]_{m,2}, \dots, [\bar{\mathbf{P}}]_{m,K} [\bar{\mathbf{Z}}]_{m,K}]^T \in \mathbb{R}^{K \times 1}, m = 1, 2, \dots, \bar{M}, \quad (33)$$

where $\bar{\mathbf{P}} \in \mathbb{R}^{\bar{M} \times K}$ denotes the statistical CSI for a finite number of \bar{M} position-rotation pairs.

Since we assume that the channel vectors of different users are independent and follow a Gaussian distribution with zero mean, each column of \mathbf{Y}_m , denoted as $[\mathbf{Y}_m]_{:,n}$, $1 \leq n \leq N$, can be treated as an independent sample following the multivariate complex Gaussian distribution based on (33), i.e.,

$$[\mathbf{Y}_m]_{:,n} \sim \mathcal{CN}(\mathbf{0}, \mathbf{X} \text{diag}(\boldsymbol{\eta}_m) \mathbf{X}^H + \sigma^2 \mathbf{I}_L). \quad (34)$$

Now, we aim to jointly determine 6DMA directional sparsity matrix $\bar{\mathbf{Z}}$ and estimate average channel power matrix $\bar{\mathbf{P}}$. This involves estimating the power state vector $\boldsymbol{\eta}_m$ from noisy observations \mathbf{Y}_m by utilizing the known pilot matrix \mathbf{X} . In general, this estimation can be formulated as a maximum likelihood (ML) problem [24], [25]. Specifically, we define $\boldsymbol{\Sigma}_m = \mathbf{X} \text{diag}(\boldsymbol{\eta}_m) \mathbf{X}^H + \sigma^2 \mathbf{I}_L$. Then, the likelihood function of \mathbf{Y}_m given $\boldsymbol{\eta}_m$ can be represented as ⁶

$$P(\mathbf{Y}_m | \boldsymbol{\eta}_m) = \prod_{n=1}^N \frac{1}{\det(\pi \boldsymbol{\Sigma}_m)} \exp(-[\mathbf{Y}_m]_{:,n}^H \boldsymbol{\Sigma}_m^{-1} [\mathbf{Y}_m]_{:,n}) \quad (35)$$

$$= \frac{1}{\det(\pi \boldsymbol{\Sigma}_m)^N} \exp(-\text{tr}(\boldsymbol{\Sigma}_m^{-1} \mathbf{Y}_m \mathbf{Y}_m^H)). \quad (36)$$

By exploiting the Gaussianity, we consider the ML estimator of $\boldsymbol{\eta}_m$. After performing normalization and simplification, we obtain the following equation:

$$f(\boldsymbol{\eta}_m) = -\ln P(\mathbf{Y}_m | \boldsymbol{\eta}_m) = \ln \det(\boldsymbol{\Sigma}_m) + \text{tr}(\boldsymbol{\Sigma}_m^{-1} \hat{\boldsymbol{\Sigma}}_m), \quad (37)$$

where $\hat{\boldsymbol{\Sigma}}_m = \frac{1}{N} \mathbf{Y}_m \mathbf{Y}_m^H$ denotes the sample covariance matrix of the received signal at the m -th candidate position/rotation pair averaged over all N antennas of the 6DMA surface. Based on (37), the ML estimation problem can be formulated as

$$\arg \min_{\boldsymbol{\eta}_m \in \mathbb{R}_+} f(\boldsymbol{\eta}_m). \quad (38)$$

The solution to (38) depends on \mathbf{Y}_m through sample covariance matrix $\frac{1}{N} \mathbf{Y}_m \mathbf{Y}_m^H$, whose size scales with L instead of N .

Next, we derive a closed-form expression for the coordinate-wise minimization of $f(\boldsymbol{\eta}_m)$ in (37). Let $k \in \{1, 2, \dots, K\}$ be the index of the coordinate being considered and ν be the update step. We define $f_k(\nu) = f(\boldsymbol{\eta}_m + \nu \mathbf{e}_k)$, where $\mathbf{e}_k \in \mathbb{R}^K$ is the k -th canonical basis vector. Using the Sherman-Morrison rank-one update identity [26], we obtain

$$(\boldsymbol{\Sigma}_m + \nu \mathbf{x}_k \mathbf{x}_k^H)^{-1} = \boldsymbol{\Sigma}_m^{-1} - \frac{\nu \boldsymbol{\Sigma}_m^{-1} \mathbf{x}_k \mathbf{x}_k^H \boldsymbol{\Sigma}_m^{-1}}{1 + \nu \mathbf{x}_k^H \boldsymbol{\Sigma}_m^{-1} \mathbf{x}_k}. \quad (39)$$

Applying the well-known determinant identity, we have

$$\det(\boldsymbol{\Sigma}_m + \nu \mathbf{x}_k \mathbf{x}_k^H) = (1 + \nu \mathbf{x}_k^H \boldsymbol{\Sigma}_m^{-1} \mathbf{x}_k) \det(\boldsymbol{\Sigma}_m). \quad (40)$$

Then, substituting (39) and (40) into (37) and taking the derivative of $f(\boldsymbol{\eta}_m)$ w.r.t. ν lead to

$$\nabla f(\nu) = \frac{\mathbf{x}_k^H \boldsymbol{\Sigma}_m^{-1} \mathbf{x}_k}{1 + \nu \mathbf{x}_k^H \boldsymbol{\Sigma}_m^{-1} \mathbf{x}_k} - \frac{\mathbf{x}_k^H \boldsymbol{\Sigma}_m^{-1} \hat{\boldsymbol{\Sigma}}_m \boldsymbol{\Sigma}_m^{-1} \mathbf{x}_k}{(1 + \nu \mathbf{x}_k^H \boldsymbol{\Sigma}_m^{-1} \mathbf{x}_k)^2}. \quad (41)$$

The solution of $\nabla f(\nu) = 0$ is thus given by

$$\nu^* = \frac{\mathbf{x}_k^H \boldsymbol{\Sigma}_m^{-1} \hat{\boldsymbol{\Sigma}}_m \boldsymbol{\Sigma}_m^{-1} \mathbf{x}_k - \mathbf{x}_k^H \boldsymbol{\Sigma}_m^{-1} \mathbf{x}_k}{(\mathbf{x}_k^H \boldsymbol{\Sigma}_m^{-1} \mathbf{x}_k)^2}. \quad (42)$$

As noted in [24], [25], to ensure that $[\boldsymbol{\eta}_m]_k$ remains positive after the update $[\boldsymbol{\eta}_m]_k \rightarrow [\boldsymbol{\eta}_m]_k + \nu$, the optimal update step ν is $\max(\nu^*, -[\boldsymbol{\eta}_m]_k)$, as demonstrated in Algorithm 1.

Once the statistical CSI for a finite number of \bar{M} position-rotation pairs, i.e., $\bar{\mathbf{P}} \in \mathbb{R}^{\bar{M} \times K}$, is estimated, the statistical CSI for any of the M position-rotation pairs in the BS site

⁶The authors of [24] have shown that although (35) is valid only for uncorrelated channels across the N antennas of the same 6DMA surface, the proposed covariance-based method still provides an accurate estimate of $\boldsymbol{\eta}_m$ as long as the channel vectors are not highly correlated, such as in line-of-sight (LoS) conditions.

Algorithm 1 Distributed Joint Directional Sparsity Detection and Channel Power (JDC) Estimation

- 1: **Input:** $\{\mathbf{Y}_m\}_{m=1}^{\bar{M}}$, \mathbf{X} , $\{\hat{\Sigma}_m = \frac{1}{N} \mathbf{Y}_m \mathbf{Y}_m^H\}_{m=1}^{\bar{M}}$, and number of iterations T .
 - 2: **Initialization:** $\{\boldsymbol{\eta}_m = \mathbf{0}, \bar{\mathbf{Z}} = \mathbf{0}\}_{m=1}^{\bar{M}}$, $\{\Sigma_m = \sigma^2 \mathbf{I}_L\}_{m=1}^{\bar{M}}$.
 - 3: For each LPU $b = 1, 2, \dots, B$, do the following steps in parallel:
 - 4: **for** $t = 1 : T$ **do**
 - 5: **for** $m = 1 : M_g$ **do**
 - 6: Select an index $k \in \{1, 2, \dots, K\}$ corresponding to the k -th element of $\boldsymbol{\eta}_m$ randomly;
 - 7: Set $\nu^* = \max \left\{ \frac{\mathbf{x}_k^H \Sigma_m^{-1} \bar{\Sigma}_m \Sigma_m^{-1} \mathbf{x}_k - \mathbf{x}_k^H \Sigma_m^{-1} \mathbf{x}_k}{(\mathbf{x}_k^H \Sigma_m^{-1} \mathbf{x}_k)^2}, -[\boldsymbol{\eta}_m]_k \right\}$;
 - 8: Update $[\boldsymbol{\eta}_m]_k = [\boldsymbol{\eta}_m]_k + \nu^*$;
 - 9: $\Sigma_m = \Sigma_m + \nu^* \mathbf{x}_k \mathbf{x}_k^H$;
 - 10: Set directional sparsity $[\bar{\mathbf{Z}}]_{m,k} = 1$ if $[\boldsymbol{\eta}_m]_k$ exceeds a given threshold $\epsilon > 0$.
 - 11: **end for**
 - 12: **end for**
 - 13: Obtain $\bar{\mathbf{P}} \in \mathbb{R}^{\bar{M} \times K}$ and $\bar{\mathbf{Z}} \in \mathbb{R}^{\bar{M} \times K}$.
 - 14: Reconstruct channel power for $\mathbf{P} \in \mathbb{R}^{M \times K}$ and directional sparsity for $\mathbf{Z} \in \mathbb{R}^{M \times K}$.
 - 15: **Output:** Estimation of $\mathbf{P} \in \mathbb{R}^{M \times K}$ and $\mathbf{Z} \in \mathbb{R}^{M \times K}$.
-

region \mathcal{C} can be reconstructed, which is formulated as a sparse signal recovery problem and solved using compressed sensing techniques [27].

We summarize the above distributed joint directional sparsity detection and channel power estimation (JDC) algorithm in Algorithm 1. Note that in Algorithm 1, all LPUs estimate the statistical CSI parameters in a parallel manner. This not only accelerates computation but also significantly reduces the computational overhead of each LPU, as the number of channels to be estimated for each LPU is reduced from M to a smaller M_g .

B. Directional Sparsity Aided Instantaneous Channel Estimation in Stage III

With the estimated directional sparsity from Stage I (see the preceding subsection) and the optimized 6DMA positions/rotations from Stage II (see Section V for details), we propose a directional sparsity-aided least-square (LS) algorithm for each LPU to estimate the instantaneous CSI from the users to its respective 6DMA surface at the optimized position/rotation in Stage III in this subsection. Note that all LPUs can estimate the instantaneous channels between the users and their respective 6DMA surfaces simultaneously in parallel. Consequently, for any LPU b , we express the received signal $\mathbf{Y}_{i_b} \in \mathbb{C}^{L \times N}$ in terms of the transmitted pilot (measurement) matrix \mathbf{X} as

$$\mathbf{Y}_{i_b} = \mathbf{X} \mathbf{H}_{i_b}^T + \mathbf{W}_{i_b}. \quad (43)$$

By vectorizing the matrix in (43), we have

$$\mathbf{y}_{i_b} = \mathbf{A} \mathbf{h}_{i_b} + \mathbf{w}_{i_b}, \quad (44)$$

TABLE I
COMPUTATIONAL COMPLEXITY COMPARISON OF DIFFERENT ALGORITHMS.

Channel Estimation Algorithm	Complexity Order
Distributed JDC (proposed)	$\mathcal{O}(L^2 K M_g)$
Distributed AMP	$\mathcal{O}(L K N M_g)$
Centralized BOMP	$\mathcal{O}(M N K L L_h)$

where $\mathbf{y}_{i_b} = \text{vec}(\mathbf{Y}_{i_b})$, $\mathbf{w}_{i_b} = \text{vec}(\mathbf{W}_{i_b})$, $\mathbf{h}_{i_b} = \text{vec}(\mathbf{H}_{i_b}^T) \in \mathbb{C}^{N K \times 1}$, and $\mathbf{A} = \mathbf{I}_K \otimes \mathbf{X} \in \mathbb{C}^{N L \times K N}$. With the known \mathbf{A} , we aim to estimate \mathbf{h}_{i_b} from \mathbf{y}_{i_b} , $b \in \mathcal{B}$.

Next, we leverage the knowledge of channel directional sparsity \mathbf{Z} estimated in the previous Stage I to improve the instantaneous channel estimation accuracy in Stage III. Specifically, we construct the support vector of \mathbf{h}_{i_b} , i.e., $\hat{\mathbf{L}}_b \in \mathbb{C}^{N K \times 1}$, based on the estimated directional sparsity indicator matrix \mathbf{Z} in Algorithm 1 as follows:

$$\hat{\mathbf{L}}_b = [\mathbf{Z}]_{i_b, :}^T \otimes \mathbf{1}_{N \times 1} \in \mathbb{C}^{N K \times 1}. \quad (45)$$

Then, let $\mathbf{A}_{\hat{\mathbf{L}}_b}$ denote the matrix composed of the corresponding columns of $\hat{\mathbf{L}}_b$ in matrix \mathbf{A} , and $\mathbf{h}_{i_b, \hat{\mathbf{L}}_b}$ denote the vector composed of the corresponding rows of $\hat{\mathbf{L}}_b$ in vector \mathbf{h}_{i_b} . Consequently, the signal in (44) can be rewritten as

$$\mathbf{y}_{i_b} = \mathbf{A}_{\hat{\mathbf{L}}_b} \mathbf{h}_{i_b, \hat{\mathbf{L}}_b} + \mathbf{w}_{i_b}. \quad (46)$$

Last, we obtain the support-restricted estimates at the b -th ($b \in \mathcal{B}$) LPU using the following LS-based rule:

$$\begin{aligned} \mathbf{h}_{i_b, \hat{\mathbf{L}}_b} &\leftarrow \arg \min_{\mathbf{h}} \|\mathbf{A}_{\hat{\mathbf{L}}_b} \mathbf{h} - \mathbf{y}_{i_b}\|_2^2, \\ \text{and } \mathbf{h}_{i_b, \hat{\mathbf{L}}_b^c} &\leftarrow 0. \end{aligned} \quad (47)$$

C. Complexity Analysis

In this subsection, we compare the computational complexity of the proposed distributed JDC algorithm with those of two CS-based algorithms adopted as benchmark, i.e., the distributed Approximate Message Passing (AMP) algorithm [28] and centralized block OMP (BOMP) algorithm [29], for estimating the 6DMA channels.

- Distributed AMP Algorithm: Each LPU uses AMP to estimate the row-sparse channel \mathbf{H}_m , $m = 1, 2, \dots, \bar{M}$ directly.
- Centralized BOMP Algorithm: The CPU first gathers signals from all LPUs, which are given by

$$\mathbf{Y} = \mathbf{X} \mathbf{H}^T + \mathbf{W}, \quad (48)$$

where $\mathbf{Y} = [\mathbf{Y}_1^T, \mathbf{Y}_2^T, \dots, \mathbf{Y}_{\bar{M}}^T]^T \in \mathbb{C}^{L \times \bar{M} N}$ and $\mathbf{W} = [\mathbf{W}_1^T, \mathbf{W}_2^T, \dots, \mathbf{W}_{\bar{M}}^T]^T \in \mathbb{C}^{L \times \bar{M} N}$. By vectorizing the received signal matrix in (48), we have

$$\mathbf{y} = \mathbf{A} \mathbf{h} + \mathbf{w}, \quad (49)$$

where $\mathbf{h} = \text{vec}(\mathbf{H}^T) \in \mathbb{C}^{\bar{M} N K \times 1}$, $\mathbf{A} = \mathbf{I}_{\bar{M} N} \otimes \mathbf{X} \in \mathbb{C}^{\bar{M} N L \times \bar{M} N K}$, $\mathbf{y} = \text{vec}(\mathbf{Y}) \in \mathbb{C}^{\bar{M} N L \times 1}$, and $\mathbf{w} = \text{vec}(\mathbf{W}) \in \mathbb{C}^{\bar{M} N L \times 1}$. Given the known \mathbf{A} , we aim to estimate \mathbf{h} from \mathbf{y} . Note that the directional sparsity indicator matrix \mathbf{Z} induces a block sparsity in \mathbf{h} . Given the noisy observation \mathbf{y} in (49), the BOMP algorithm [29] is then used to estimate the block-sparse channel \mathbf{h} .

We assume that the computational complexity is dominated by the required number of real-valued multiplications. The

computational complexity of the centralized BOMP algorithm is $\mathcal{O}(\overline{M}NKLL_h)$ [30], where L_h denotes the number of non-zero blocks in \mathbf{h} . Besides, the computational complexity of the distributed AMP algorithm is $\mathcal{O}(LKNM_g)$ [28]. In contrast, the computational complexity of our proposed distributed JDC algorithm can be shown to be $\mathcal{O}(L^2KM_g)$. In Table I, we summarize the computational complexities of the considered schemes. We observe that the proposed distributed JDC algorithm has a significantly lower computational complexity as compared to the other two benchmarks, and its complexity does not increase with the number of antennas per 6DMA surface, N .

V. CHANNEL POWER-BASED 6DMA POSITION AND ROTATION OPTIMIZATION IN STAGE II

After obtaining the estimate of the average channel power matrix \mathbf{P} from the distributed LPUs in Stage I, the CPU optimizes the positions/rotations of all B 6DMA surfaces (i.e., the position/rotation selection vector \mathbf{s}) in Stage II to maximize the ergodic sum rate upper bound $\bar{C}(\mathbf{s})$, subject to the practical movement constraints. Accordingly, the optimization problem is formulated as follows:

$$(P1) \quad \max_{\mathbf{s}} \sum_{k=1}^K \log_2 \left(1 + \frac{p}{\sigma^2} \sum_{m=1}^M [\mathbf{s}]_m [\mathbf{P}]_{m,k} \right) \quad (50a)$$

$$\text{s.t. } \mathbf{1}^T \mathbf{s} = B, \quad (50b)$$

$$\mathbf{e}_i^T(\mathbf{s}) \mathbf{D} \mathbf{e}_j(\mathbf{s}) \geq d_{\min}, \quad i \neq j, \forall i, j \in \mathcal{B}, \quad (50c)$$

$$[\mathbf{s}]_i \in \{0, 1\}, \quad i = 1, 2, \dots, M, \quad (50d)$$

where $\mathbf{e}_i(\mathbf{s}) \in \mathbb{R}^{M \times 1}$ is a vector with a single one at the index of the i -th non-zero entry of \mathbf{s} and zeros elsewhere. For example, if $\mathbf{s} = [1, 0, 0, 1, 0]^T$, then $\mathbf{e}_1 = [1, 0, 0, 0, 0]^T$ and $\mathbf{e}_2 = [0, 0, 0, 1, 0]^T$. As discussed in Section II-A, constraint (50c) prevents overlapping and coupling between 6DMA surfaces. Constraints (50b) and (50d) ensure that no candidate position-rotation pair is selected by more than one 6DMA surface. Note that for simplicity, this paper assumes that discrete candidate position-rotation pairs are generated uniformly on a sphere inside \mathcal{C} (see Section VI for details), so the rotation constraints in (5) and (6) are naturally satisfied.

We can see that (P1) is a non-convex integer programming problem that becomes progressively more challenging to solve optimally as the value of M increases. In order to tackle this issue, we initially employ linear programming relaxation by relaxing the binary variables to take on continuous values within the range of $[0, 1]$ [12]. Then, inspired by the efficiency and effectiveness of particle swarm optimization (PSO) algorithms [31], we introduce a channel power-based PSO technique for optimizing 6DMA positions and rotations. The proposed algorithm is described in Algorithm 2, which systematically updates many particles, each characterized by their position $\mathbf{s} \in \mathbb{R}^{M \times 1}$ and velocity $\mathbf{v} \in \mathbb{R}^{M \times 1}$.

We aim to minimize $\bar{C}(\mathbf{s})$, which serves as the fitness function. However, due to the constraints in (P1), the fitness function must be adjusted [31]. To satisfy constraints (50b)–(50d), we incorporate an adaptive penalty factor, resulting in the following fitness function:

$$\mathcal{F}(\mathbf{s}) = \bar{C}(\mathbf{s}) + \tau \mathcal{Q}(\mathbf{s}), \quad (51)$$

where τ denotes positive penalty parameter, and $\mathcal{Q}(\mathbf{s})$ is the penalty factor for the infeasible particles, which is defined as

$$\mathcal{Q}(\mathbf{s}) = \left| \left\{ (i, j) \mid \mathbf{e}_i(\bar{\mathbf{s}})^T \mathbf{D} \mathbf{e}_j(\bar{\mathbf{s}}) < d_{\min}, 1 \leq i < j \leq B \right\} \right|_c + |B - \mathbf{1}^T \bar{\mathbf{s}}|, \quad (52)$$

where $\bar{\mathbf{s}} = \text{round}(\mathbf{s})$.

In iteration t , the position and velocity of the ι -th particle are denoted by $\mathbf{s}_\iota^{(t)}$ and $\mathbf{v}_\iota^{(t)}$, respectively. As detailed in Algorithm 2, during initialization, we randomly set the positions and velocities of I particles as follows:

$$\mathcal{R}^{(0)} = \{\mathbf{s}_1^{(0)}, \mathbf{s}_2^{(0)}, \dots, \mathbf{s}_I^{(0)}\}, \quad (53)$$

$$\mathcal{V}^{(0)} = \{\mathbf{v}_1^{(0)}, \mathbf{v}_2^{(0)}, \dots, \mathbf{v}_I^{(0)}\}. \quad (54)$$

Let $\mathbf{s}_{\iota, \text{pbest}}$ denote the best position of the ι -th particle, and $\mathbf{s}_{g\text{best}}$ represent the global best position. In the initial stage, we set $\mathbf{s}_{\iota, \text{pbest}} = \mathbf{s}_\iota^{(0)}$, $1 \leq \iota \leq I$, and

$$\mathbf{s}_{g\text{best}} = \arg \min_{\mathbf{s}_i^{(0)}} \left\{ \mathcal{F}(\mathbf{s}_1^{(0)}), \mathcal{F}(\mathbf{s}_2^{(0)}), \dots, \mathcal{F}(\mathbf{s}_I^{(0)}) \right\}. \quad (55)$$

For each iteration t , the velocity of each particle ι is updated as [31]

$$\mathbf{v}_\iota^{(t+1)} = \kappa \mathbf{v}_\iota^{(t)} + c_1 \tau_1 (\mathbf{s}_{\iota, \text{pbest}} - \mathbf{s}_\iota^{(t)}) + c_2 \tau_2, \quad (56)$$

where c_1 and c_2 are the individual and global learning factors, τ_1 and τ_2 are random parameters uniformly distributed in $[0, 1]$, and κ is the inertia weight [31]. In each iteration t , the position of each particle ι is updated as follows:

$$\mathbf{s}_\iota^{(t+1)} = \mathbf{s}_\iota^{(t)} + \mathbf{v}_\iota^{(t)}. \quad (57)$$

Next, we evaluate each particle's fitness using (51) and compare it with the fitness values at its local and global best positions, as shown in lines 10-15 of Algorithm 2. The global best fitness value is non-increasing, i.e., $\mathcal{F}(\mathbf{s}_{g\text{best}}^{t+1}) \leq \mathcal{F}(\mathbf{s}_{g\text{best}}^t)$, which ensures convergence. The complexity of PSO is given by $\mathcal{O}(IT_{\text{PSO}})$, where T_{PSO} is the maximum number of iterations of Algorithm 2.

VI. SIMULATION RESULTS

In this section, numerical results are provided to validate the performance of our proposed 6DMA channel estimation algorithms as well as the statistical channel power based 6DMA position/rotation optimization. Unless stated otherwise, we set $N = 4$, meaning each 6DMA surface is equipped with a 2×2 UPA with antenna elements spaced $\lambda/2$. The number of 6DMA surfaces is $B = 16$, and the number of candidate position-rotation pairs is $M = 256$. The carrier frequency is 2.4 GHz and the wavelength is $\lambda = 0.125$ m. We set the number of multi-path components per user as $\Gamma_k = 100, \forall k$. The multi-path channels per user are generated by firstly randomly generating the user's location in the BS's coverage area (assumed to be a spherical annulus region \mathcal{L} with radial distances from 30 m to 200 m from the CPU center) and then generating random scatterers uniformly within a circle centered at the user's location and with the radius equal to 1 m. This coverage region \mathcal{L} consists of three distinct hotspot sub-regions, \mathcal{L}_v for $v = 1, 2, 3$, and a regular user sub-region \mathcal{L}_0 , such that $\mathcal{L} = \mathcal{L}_0 \cup (\cup_{v=1}^3 \mathcal{L}_v)$. The hotspot sub-regions \mathcal{L}_1 , \mathcal{L}_2 , and \mathcal{L}_3 are 3D spheres centered at 100 m, 60 m, and 40 m from the CPU, with radii of 15 m, 10 m, and 5

Algorithm 2 Channel Power-Based 6DMA PSO Algorithm for Solving (P1).

- 1: **Input:** $B, N, I, K, T_{\text{PSO}}$, and channel power estimate $\hat{\mathbf{P}}$.
 - 2: **Output:** Position/rotation selection vector \mathbf{s} .
 - 3: Initialize particles with positions $\mathcal{R}^{(0)}$ and velocities $\mathcal{V}^{(0)}$ according to (53) and (54), respectively.
 - 4: Obtain the local best position $\mathbf{s}_{\iota, \text{pbest}} = \mathbf{s}_{\iota}^{(0)}$ for $1 \leq \iota \leq I$ and the global best position according to (55).
 - 5: **for** $t = 1$ to T_{PSO} **do**
 - 6: **for** $\iota = 1$ to I **do**
 - 7: Update the velocity of particle ι according to (56);
 - 8: Update the position of particle ι according to (57);
 - 9: Evaluate the fitness value of particle ι , i.e., $\mathcal{F}(\mathbf{s}_{\iota}^{(t)})$ and update it according to (51);
 - 10: **if** $\mathcal{F}(\mathbf{s}_{\iota}^{(t)}) > \mathcal{F}(\mathbf{s}_{\iota, \text{pbest}})$ **then**
 - 11: Update $\mathbf{s}_{\iota, \text{pbest}} \leftarrow \mathbf{s}_{\iota}^{(t)}$
 - 12: **end if**
 - 13: **if** $\mathcal{F}(\mathbf{s}_{\iota}^{(t)}) > \mathcal{F}(\mathbf{s}_{g\text{best}})$ **then**
 - 14: Update $\mathbf{s}_{g\text{best}} \leftarrow \mathbf{s}_{\iota}^{(t)}$
 - 15: **end if**
 - 16: **end for**
 - 17: **end for**
 - 18: Obtain the optimized rotation and position vector $\mathbf{s} = \mathbf{s}_{g\text{best}}$.
 - 19: Return $\mathbf{s} = \text{round}(\mathbf{s})$.
-

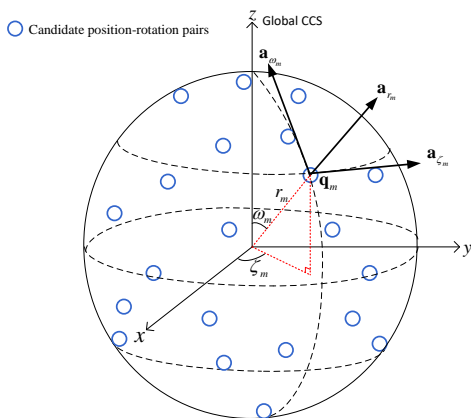


Fig. 5. Candidate position-rotation pairs for 6DMA surfaces.

m , respectively. Users are distributed in these areas according to a homogeneous Poisson point process, with the proportion of regular users given by $\varpi = \frac{\text{number of regular users}}{\text{total number of users}} = 0.3$. The effective antenna gain $A(\hat{\theta}_{b,\iota,k}, \hat{\phi}_{b,\iota,k})$ in (14) is set as the half-space directive antenna pattern [32], [33].

For simplicity, we assume that discrete candidate position-rotation pairs are generated uniformly on a sphere. As shown in Fig. 5, we start by making $M > B$ candidate positions evenly spread out on the biggest spherical surface that fits in the 6DMA-BS site space \mathcal{C} . We change the Cartesian coordinates of each possible position $\mathbf{q}_m, m \in \mathcal{M}$ to spherical coordinates (r_m, w_m, ζ_m) with r_m , w_m , and ζ_m being the position's radius, polar angle, and azimuthal angle, respectively. We can then determine a unique rotation angle for each

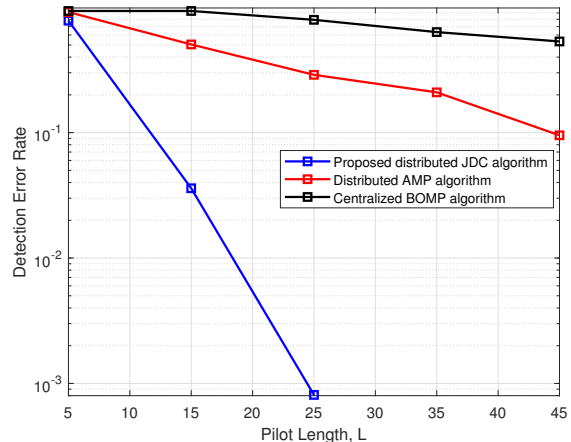


Fig. 6. The detection error rate versus pilot length with $K = 50$ users.

position based on the basis vectors of the spherical coordinates, denoted by $(\mathbf{a}_{r_m}, \mathbf{a}_{w_m}, \mathbf{a}_{\zeta_m})$. For further details, please refer to [11].

Now, we introduce the performance metrics for directional sparsity estimation, average channel power estimation, and instantaneous channel estimation. For directional sparsity detection, we adopt the detection error rate as the performance metric. The detection error rate is defined as the sum of the missed detection probability, which is the probability that a user has non-zero channels with a candidate position/rotation pair but is declared to have zero channels with it, and the false-alarm probability, which is the probability that a user has zero channels with a 6DMA position/rotation pair but is declared to have non-zero channels with it.

The performance of the average channel power estimation in Stage I is evaluated by the normalized mean square error (NMSE), which is defined as $\text{NMSE}_p = \mathbb{E} \left(\frac{\|\mathbf{P} - \hat{\mathbf{P}}\|_F^2}{\|\mathbf{P}\|_F^2} \right)$, where $\hat{\mathbf{P}}$ denotes the estimated value of channel power matrix \mathbf{P} . Similarly, the performance of the instantaneous CSI estimation in Stage III is evaluated by another NMSE, which is defined as $\text{NMSE}_c = \mathbb{E} \left(\frac{\|\mathbf{h} - \hat{\mathbf{h}}\|_2^2}{\|\mathbf{h}\|_2^2} \right)$, where $\hat{\mathbf{h}}$ denotes the estimated value of instantaneous channel vector \mathbf{h} .

We first conduct simulations to validate the effectiveness of the proposed JDC algorithm (Algorithm 1) for directional sparsity estimation. We also compare the proposed JDC algorithm with two baseline schemes (as discussed in Section IV-D): distributed AMP algorithm [28] and centralized BOMP algorithm [29]. Fig. 6 shows the estimation performance versus the length of the pilot sequences, L . From this figure, we can observe that the detection error rates of all the considered algorithms decrease as the pilot length increases. We can also see that the proposed JDC algorithm reduces the required length of the required pilots for achieving a desired accuracy of directional sparsity estimation compared with the two benchmark schemes. Fig. 6 also shows that the proposed JDC algorithm is more suitable for small L in which case AMP and BOMP may not work well.

In Fig. 7 we compare the proposed JDC algorithm with AMP and BOMP for average channel power estimation, as

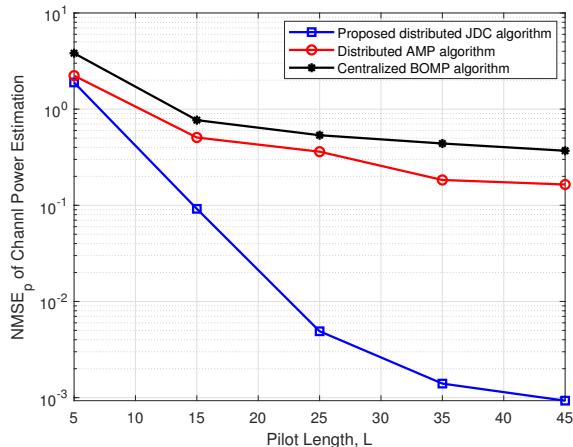


Fig. 7. The NMSE of channel power estimation versus pilot length with $K = 50$ users.

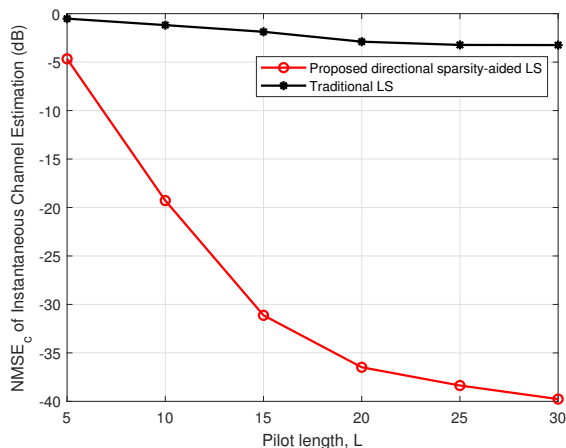


Fig. 8. The NMSE of instantaneous channel estimation versus pilot length with $K = 30$ users.

the pilot length L increases. We observe that increasing L decreases the NMSE for channel power estimation for the proposed JDC algorithm much faster compared to the two benchmark schemes.

Next, we plot the NMSE for instantaneous CSI estimation as a function of the length of pilot sequence L in Fig. 8. As L increases, it is observed that the NMSEs of the proposed directional sparsity-aided LS algorithm and the traditional LS algorithm (which does not use the estimated directional sparsity in (45)) both decrease, which is expected. However, the proposed directional sparsity-aided LS algorithm achieves higher estimation accuracy than the conventional LS algorithm. Moreover, the NMSE gap between the two algorithms increases with L . To achieve the same estimation accuracy, the proposed directional sparsity-aided LS algorithm requires much lower pilot overhead (i.e., L) than the benchmark scheme. This implies that the effective data rates of users can be significantly increased during Stage III of the proposed protocol.

Next, we conduct simulations to validate the effectiveness of the proposed channel power-based 6DMA position and

rotation optimization method. We compare the proposed channel power-based 6DMA PSO algorithm (Algorithm 2) with the following five baseline schemes, where the total number of antennas for each benchmark scheme is set the same as for the proposed scheme. For the proposed and benchmark schemes, we calculate the sum rate by averaging over 20 channel realizations with the optimized antenna positions and rotations.

- Perfect CSI-based continuous 6DMA alternating optimization (AO) [11]: We assume that the instantaneous CSI is perfectly known and AO proposed in [11] is used to optimize continuous antenna positions and rotations.
- Perfect CSI-based discrete 6DMA PSO: We assume that the instantaneous CSI is perfectly known and PSO is used to optimize the discrete antenna positions and rotations.
- Channel power-based discrete 6DMA random-max sampling (RMS): Based on the estimated channel power, we generate 100 random samples each consisting of B different discrete position-rotation pairs and then choose the best sample which yields the highest sum rate.
- FPA with perfect CSI: We consider a conventional three-sector BS (which can be regarded as a special case of the 6DMA-BS with $B = 3$ and approximately $\lceil \frac{NB}{3} \rceil$ antennas on each surface), where each sector antenna surface covers roughly 120° horizontally. The 3D locations and 3D rotations of all antennas are fixed.
- Fluid/movable antenna with perfect CSI [15], [34], [35]: We consider again a three-sector BS. The rotations of all antennas remain unchanged, while we apply the AO-based algorithm proposed in [11] to optimize the continuous positions of the antennas within each 2D sector antenna surface.

Fig. 9 shows the sum rate achieved by the proposed channel power-based 6DMA PSO algorithm and the baseline schemes versus the user transmit power. It is observed that the sum rate increases with the transmit power. The performance of the proposed algorithm is very close to that of 6DMA PSO with perfect CSI. This is because overcoming deep fading in instantaneous small-scale channels results in minimal gain, and the increase in sum rate is primarily determined by channel power. This result demonstrates the effectiveness of using average channel power (i.e., statistical CSI instead of instantaneous CSI) for 6DMA position and rotation optimization. However, one can observe that the proposed algorithm suffers a performance loss compared to the AO algorithm with continuous positions and rotations [11]. This is because the discrete position/rotation adjustments of the 6DMA surfaces limit their spatial DoFs for adapting to the user channel distributions. It is also observed that the RMS approach yields the worst 6DMA sum rate performance, which, however, is still significantly better than that of the FPA and fluid/movable antenna systems, even with perfect CSI.

In Fig. 10, we compare the sum rate for the considered schemes versus the number of users. First, it is observed that the proposed channel power-based 6DMA PSO algorithm performs better than the RMS, FPA, and fluid/movable antenna systems. This is due to the fact that the 6DMA scheme has

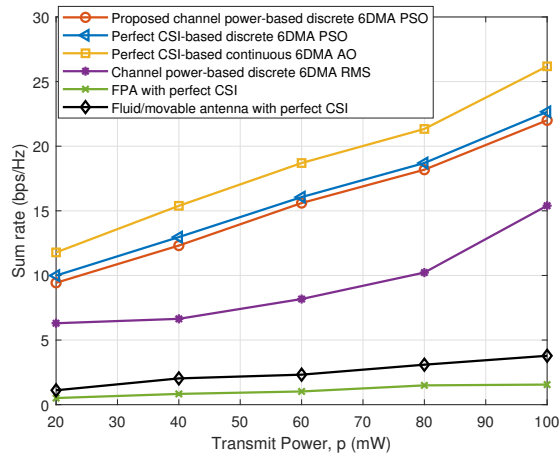


Fig. 9. Sum rate versus transmit power for $K = 30$ users.

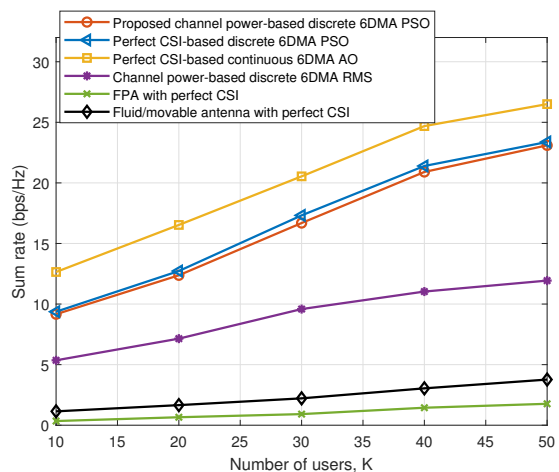


Fig. 10. Sum rate versus number of users for transmit power $p = 60$ mW.

more spatial DoFs and can deploy the antenna resources more efficiently to match the user spatial distribution. On the other hand, the fluid/movable antenna scheme can only adjust the antenna positions within 2D surfaces. Second, it is observed that the performance gaps become larger as the number of users increases. This suggests that the proposed 6DMA-BS design and algorithms are particularly advantageous in scenarios with higher network loads and thus being more interference-limited.

VII. CONCLUSIONS

This paper proposed a distributed 6DMA processing architecture to reduce the centralized processing complexity by equipping each 6DMA surface with a local LPU. Under the new hybrid architecture with the CPU and distributed LPUs, we presented a practical protocol for operating the BS equipped with 6DMA surfaces. We designed a joint directional sparsity detection and channel power estimation algorithm for statistical CSI acquisition, as well as a directional sparsity-aided instantaneous channel estimation algorithm. Using the estimated channel average power, we further designed a statistical channel power-based antenna position and rotation

optimization algorithm to maximize the average sum-rate of all users. Extensive simulation results were presented for various practical setups, showing that the proposed channel estimation algorithms achieve higher estimation accuracy than existing schemes while reducing the pilot overhead and also verifying the effectiveness of the practical channel power-based 6DMA position/rotation optimization scheme.

REFERENCES

- [1] E. G. Larsson, O. Edfors, F. Tufvesson, and T. L. Marzetta, "Massive MIMO for next generation wireless systems," *IEEE Commun. Mag.*, vol. 52, no. 2, pp. 186–195, Feb. 2014.
- [2] A. L. Swindlehurst, E. Ayanoglu, P. Heydari, and F. Capolino, "Millimeter-wave massive MIMO: the next wireless revolution?" *IEEE Commun. Mag.*, vol. 52, no. 9, pp. 56–62, Sep. 2014.
- [3] E. Jorswieck and H. Boche, "Channel capacity and capacity-range of beamforming in MIMO wireless systems under correlated fading with covariance feedback," *IEEE Trans. Wireless Commun.*, vol. 3, no. 5, pp. 1543–1553, Sep. 2004.
- [4] H. Q. Ngo, A. Ashikhmin, H. Yang, E. G. Larsson, and T. L. Marzetta, "Cell-free massive MIMO versus small cells," *IEEE Trans. Wireless Commun.*, vol. 16, no. 3, pp. 1834–1850, Mar. 2017.
- [5] Z. Wang, J. Zhang, H. Du, D. Niyato, S. Cui, B. Ai, M. Debbah, K. B. Letaief, and H. V. Poor, "A tutorial on extremely large-scale MIMO for 6G: Fundamentals, signal processing, and applications," *IEEE Commun. Surv. Tutorials.*, pp. 1–1, Jan. 2024.
- [6] H. Lu and Y. Zeng, "Communicating with extremely large-scale array/surface: Unified modeling and performance analysis," *IEEE Trans. Wireless Commun.*, vol. 21, no. 6, pp. 4039–4053, Jun. 2022.
- [7] C. Huang, A. Zappone, G. C. Alexandropoulos, M. Debbah, and C. Yuen, "Reconfigurable intelligent surfaces for energy efficiency in wireless communication," *IEEE Trans. Wireless Commun.*, vol. 18, no. 8, pp. 4157–4170, Aug. 2019.
- [8] X. Shao and R. Zhang, "Target-mounted intelligent reflecting surface for secure wireless sensing," *IEEE Trans. Wireless Commun.*, early access, Feb. 2024.
- [9] X. Shao, C. You, W. Ma, X. Chen, and R. Zhang, "Target sensing with intelligent reflecting surface: Architecture and performance," *IEEE J. Sel. Areas Commun.*, vol. 40, no. 7, pp. 2070–2084, Jul. 2022.
- [10] Q. Wu *et al.*, "Intelligent surfaces empowered wireless network: Recent advances and the road to 6G," *Proc. IEEE*, pp. 1–40, 2024.
- [11] X. Shao, Q. Jiang, and R. Zhang, "6D movable antenna based on user distribution: Modeling and optimization," *arXiv preprint arXiv:2403.08123*, Mar. 2024.
- [12] X. Shao, R. Zhang, Q. Jiang, and R. Schober, "6D movable antenna enhanced wireless network via discrete position and rotation optimization," *arXiv preprint arXiv:2403.17122*, Mar. 2024.
- [13] X. Shao and R. Zhang, "6DMA enhanced wireless network with flexible antenna position and rotation: Opportunities and challenges," *arXiv preprint arXiv:2406.06064*, 2024.
- [14] X. Shao, R. Zhang, and R. Schober, "Exploiting six-dimensional movable antenna for wireless sensing," *arXiv preprint arXiv:2409.01965*, 2024.
- [15] W. K. New, K.-K. Wong, H. Xu, K.-F. Tong, and C.-B. Chae, "Fluid antenna system: New insights on outage probability and diversity gain," *IEEE Trans. Wireless Commun.*, vol. 23, no. 1, pp. 128–140, Jan. 2024.
- [16] Z. Xiao, S. Cao, L. Zhu, Y. Liu, B. Ning, X.-G. Xia, and R. Zhang, "Channel estimation for movable antenna communication systems: A framework based on compressed sensing," *IEEE Trans. Wireless Commun.*, pp. 1–1, 2024.
- [17] W. Mei, X. Wei, B. Ning, Z. Chen, and R. Zhang, "Movable-antenna position optimization: A graph-based approach," *IEEE Wireless Commun. Lett.*, pp. 1–1, Apr. 2024.
- [18] Z. Zhang, J. Zhu, L. Dai, and R. W. Heath, "Successive bayesian reconstructor for FAS channel estimation," in *IEEE Wireless Commun. Net. Conf. (WCNC)*. IEEE, 2024, pp. 1–5.
- [19] K. Li, R. R. Sharan, Y. Chen, T. Goldstein, J. R. Cavallaro, and C. Studer, "Decentralized baseband processing for massive MU-MIMO systems," *IEEE J. Emerg. Sel. Topics Circuits Syst.*, vol. 7, no. 4, pp. 491–507, 2017.
- [20] Y. Xu, B. Wang, E. Song, Q. Shi, and T.-H. Chang, "Low-complexity channel estimation for massive MIMO systems with decentralized baseband processing," *IEEE Trans. Signal Process.*, vol. 71, pp. 2728–2743, 2023.

- [21] Y. Xu, E. G. Larsson, E. A. Jorswieck, X. Li, S. Jin, and T.-H. Chang, "Distributed signal processing for extremely large-scale antenna array systems: State-of-the-art and future directions," *arXiv preprint arXiv:2407.16121*, 2024.
- [22] J. Diebel *et al.*, "Representing attitude: Euler angles, unit quaternions, and rotation vectors," *Matrix*, vol. 58, no. 15-16, pp. 1–35, 2006.
- [23] D. Tse and P. Viswanath, *Fundamentals of Wireless Communication*. Cambridge University Press, 2005.
- [24] Z. Chen, F. Sofrabi, Y.-F. Liu, and W. Yu, "Covariance based joint activity and data detection for massive random access with massive MIMO," in *IEEE Intern. Conf. Commun. (ICC)*, May 2019, pp. 1–6.
- [25] X. Shao, X. Chen, D. W. K. Ng, C. Zhong, and Z. Zhang, "Cooperative activity detection: Sourced and unsourced massive random access paradigms," *IEEE Trans. Signal Process.*, vol. 68, pp. 6578–6593, 2020.
- [26] J. Sherman and W. J. Morrison, "Adjustment of an inverse matrix corresponding to a change in one element of a given matrix," *The Annals of Mathematical Statistics*, vol. 21, no. 1, pp. 124–127, 1950.
- [27] Q. Jiang, X. Shao, and R. Zhang, "6DMA optimization based on statistical CSI," *submit to IEEE for possible publication*, 2024.
- [28] L. Liu and W. Yu, "Massive connectivity with massive MIMO part I: Device activity detection and channel estimation," *IEEE Trans. Signal Process.*, vol. 66, no. 11, pp. 2933–2946, Jun. 2018.
- [29] Y. C. Eldar, P. Kuppinger, and H. Bolcskei, "Block-sparse signals: Uncertainty relations and efficient recovery," *IEEE Trans. Signal Process.*, vol. 58, no. 6, pp. 3042–3054, 2010.
- [30] Y. You, L. Zhang, M. Yang, Y. Huang, X. You, and C. Zhang, "Structured OMP for IRS-assisted mmwave channel estimation by exploiting angular spread," *IEEE Trans. Veh. Technol.*, vol. 71, no. 4, pp. 4444–4448, Apr. 2022.
- [31] M. Clerc and J. Kennedy, "The particle swarm-explosion, stability, and convergence in a multidimensional complex space," *IEEE Trans. Evol. Comput.*, vol. 6, no. 1, pp. 58–73, 2002.
- [32] 3GPP, "Technical specification group radio access network; study on 3D channel model for LTE," *3rd Generation Partnership Project (3GPP), TR 36.873 V12.4.0*, 2017.
- [33] Y. Zhang, X. Shao, H. Li, B. Clerckx, and R. Zhang, "Full-space wireless sensing enabled by multi-sector intelligent surfaces," *arXiv preprint arXiv:2406.15945*, 2024.
- [34] Y. Wu, D. Xu, D. W. K. Ng, W. Gerstacker, and R. Schober, "Movable antenna-enhanced multiuser communication: Optimal discrete antenna positioning and beamforming," in *IEEE Global Commun. Conf. (GLOBECOM)*, Dec. 2023, pp. 1–6.
- [35] W. Ma, L. Zhu, and R. Zhang, "Multi-beam forming with movable-antenna array," *IEEE Commun. Lett.*, vol. 28, no. 3, pp. 697–701, Mar. 2024.